



Does lithology influence relative paleointensity records? a statistical analysis on South Atlantic pelagic sediments

Christine Franke^{a,b,*}, Daniela Hofmann^a, Tilo von Dobeneck^{a,b}

^a Department of Geosciences, University of Bremen, P.O. Box 330 440, D-28334 Bremen, Germany

^b Paleomagnetic Laboratory 'Fort Hoofddijk', Utrecht University, Budapestlaan 17, 3584 CD Utrecht, The Netherlands

Received 24 November 2003

Abstract

The relative paleointensity (RPI) method assumes that the intensity of post depositional remanent magnetization (PDRM) depends exclusively on the magnetic field strength and the concentration of the magnetic carriers. Sedimentary remanence is regarded as an equilibrium state between aligning geomagnetic and randomizing interparticle forces. Just how strong these mechanical and electrostatic forces are, depends on many petrophysical factors related to mineralogy, particle size and shape of the matrix constituents. We therefore test the hypothesis that variations in sediment lithology modulate RPI records. For 90 selected Late Quaternary sediment samples from the subtropical and subantarctic South Atlantic Ocean a combined paleomagnetic and sedimentological dataset was established. Misleading alterations of the magnetic mineral fraction were detected by a routine Fe/ κ test (Funk, J., von Dobeneck, T., Reitz, A., 2004. Integrated rock magnetic and geochemical quantification of redoxomorphic iron mineral diagenesis in Late Quaternary sediments from the Equatorial Atlantic. In: Wefer, G., Mulitza, S., Ratmeyer, V. (Eds.), *The South Atlantic in the Late Quaternary: reconstruction of material budgets and current systems*. Springer-Verlag, Berlin/Heidelberg/New York/Tokyo, pp. 239–262). Samples with any indication of suboxic magnetite dissolution were excluded from the dataset. The parameters under study include carbonate, opal and terrigenous content, grain size distribution and clay mineral composition. Their bi- and multivariate correlations with the RPI signal were statistically investigated using standard techniques and criteria. While several of the parameters did not yield significant results, clay grain size and chlorite correlate weakly and opal, illite and kaolinite correlate moderately to the NRM/ARM signal used here as a RPI measure. The most influential single sedimentological factor is the kaolinite/illite ratio with a Pearson's coefficient of 0.51 and 99.9% significance. A three-member regression model suggests that matrix effects can make up over 50% of the observed RPI dynamics.

© 2004 Elsevier B.V. All rights reserved.

Keywords: Relative paleointensity; PDRM; Sediment lithology; Statistical analysis; South Atlantic

1. Introduction

High-resolution records of the paleointensity of the Earth's magnetic field have been successfully obtained from marine (Roberts et al., 1997; Valet and

* Corresponding author. Tel.: +49 421 218 8922;

fax: +49 421 218 8671.

E-mail address: cfranke@uni-bremen.de (C. Franke).

URL: <http://www.geophysik.uni-bremen.de/>,

<http://www.geo.uu.nl/~forth> (C. Franke).

Meynardier, 1993; Tauxe and Shackleton, 1994) and lacustrine sediment (Creer and Morris, 1996; Nowaczyk et al., 2001) sequences. These so-called ‘relative paleointensities’ (RPI) are determined by normalizing the natural remanent magnetisation (NRM) by the concentration of the magnetic carriers, quantified by parameters such as anhysteretic remanent magnetization (ARM), isothermal remanent magnetization (IRM) or magnetic susceptibility (κ) (Verosub, 1977; Kent, 1982; Tauxe, 1993).

The most widely accepted relative paleointensity reference for the last 800 kyr is the Sint-800 record (Guyodo and Valet, 1999), a global composite of 33 marine records. The RPI records used for this stack correlate well with each other, but not with paleoclimate, and therefore seem to carry a nearly unbiased paleointensity signal. However, on a global scale, very little sediments show such coherent patterns in RPI. In practice, many RPI records routinely obtained from pelagic sediments deviate partly or fully from Sint-800 for mostly unknown reasons. Regionally confined sets of RPI records with similar lithology typically match considerably well internally, but may correlate poorly to records of different origin and composition (Tauxe and Wu, 1990). In some cases, rock magnetic and diagenetic effects are responsible, but it has also been observed that the lithology of the sediment matrix appears to have an influence on the character of the RPI signal (Creer and Morris, 1996).

Laboratory resedimentation experiments by Lu et al. (1990) and Lu (1992) have shown that clay mineralogy and pore water salinity strongly affect PDRM intensity. Lower RPI values result from higher clay mineral, in particular kaolinite, concentration as well as from higher salinity. The authors explain the influence of mineral-dependent surface charges and interparticle forces on magnetic particle alignment by a so-called ‘heterocoagulation model’.

Here, we take an analytical and statistical approach to investigate the importance of such ‘matrix effects’ under natural conditions. RPI data from various deep-sea sediments that were sampled across the frontal systems of the subtropical and subantarctic South Atlantic are compared. The six sites are regionally so well confined, that they should have experienced the same paleofield history, in particular if a (fairly small) dipole based latitudinal correction is applied. These very continent-far locations on the western

slope of the Mid-Atlantic ridge receive mainly eolian magnetic mineral input from Patagonian sources (Schmieder et al., 2000) and therefore carry similar magnetic mineral inventories. A detailed environmental magnetic study of this region by Hofmann and Fabian is in preparation. Characteristic differences between the RPI values should therefore reflect the influence of the sediment matrix on magnetic particle alignment.

Extensive sedimentological data were collected for a total of 90 samples from six Late Quaternary sediment series. The sediment matrix was characterized with respect to lithology and grain size. Using bi- and multi-variate statistics, we challenge the prevailing working (and ‘null’) hypothesis that the mentioned sediment characteristics have no influence on PDRM intensity. In more mathematical terms, we investigate, whether RPI records can be expressed as a product of paleofield intensity, magnetic carrier concentration and a specific ‘lithology factor’ introducing the influence of the sediment matrix.

2. Material and methods

The proposed paleomagnetic and sedimentological investigations require undisturbed oxic sediments with differing lithologies, but a common field history, hence a narrow spatial distribution. For the deposits of the selected investigation area, the subtropical and subantarctic South Atlantic, all these conditions are largely fulfilled.

The material originates from the western slope of the Mid-Atlantic Ridge (MAR) between 44–32°S and 25–22°W and was taken by gravity coring during the R/V Meteor Cruise M 46/4 (Collaborative Research Center 261, University of Bremen) in March 2000 (Fig. 1). Six out of 29 recovered sediment cores (Table 1) from water depths of 3500–4300 m were selected on basis of their distinct physical properties (porosity, p-wave velocity, magnetic susceptibility and color reflectance) investigated by shipboard logging techniques (Wefer et al., 2001). According to shipboard core descriptions (Wefer et al., 2001), all sediment series appear to be free from disturbances such as hiati or turbidities. Due to a strong southwards increase in primary productivity, there is a tenfold N–S increase in sedimentation rate (0.43–4.56 cm/kyr) from the olig-

Table 1
Core information

Core	Longitude (S)	Latitude (W)	Water depth (m)	Core length (m)	Sedimentation rate (cm/kyr)
GeoB 6428-1	32°30.60	24°14.91	4015	7.26	0.43
GeoB 6425-2	33°49.51	23°35.24	4352	10.73	1.05
GeoB 6422-1	35°42.45	22°44.01	3972	5.32	1.77
GeoB 6407-1	42°02.70	19°30.00	3384	5.36	1.76
GeoB 6405-6	42°00.00	21°51.19	3862	11.94	4.56
GeoB 6408-4	43°00.00	20°26.46	3817	10.55	3.77

otrophic subtropical to the mesotrophic subantarctic South Atlantic.

The six selected cores fall into three different lithological categories; the two northernmost cores from the oligotrophic subtropics (GeoB 6425-2 and 6428-1) have elevated clay mineral contents. The two cores at the subtropical front (GeoB 6407-1 and 6422-1) mostly contain calcareous nannofossil ooze with some foraminifers due to higher primary productivity. The two southernmost cores (GeoB 6405-6 and 6408-4) are under influence of the subantarctic front and have an additional siliceous component contributed by diatoms. In the following, these three sediment types are called clay bearing, foram bearing, and diatom bearing nannofossil oozes. A total of 90 discrete samples, about 15 per core, were taken from maxima and minima of the

marine isotope stages 2–8, always from matching age positions back to 280 ka.

The age models of the two northernmost sediment cores GeoB 6425-2 and GeoB 6428-1 (Schmieder, 2004) were based on a correlation of susceptibility κ to the ‘Subtropical South Atlantic Susceptibility Stack’ (SUSAS) established by von Dobeneck and Schmieder (1999). The age models of cores GeoB 6405-6, GeoB 6407-1, GeoB 6422-1 and GeoB 6408-4 depend on a multi-parameter correlation (Hofmann et al., in preparation) of κ and element logs, which were tied to the SUSAS and SPECMAP stack (Imbrie et al., 1984). The maxima and minima of the susceptibility signal follow Quaternary climate cycles and correlate very well with available $\delta^{18}\text{O}$ isotope records (Donner, unpublished data).

The total carbonate content (Müller, unpublished data) was determined with a Herateus CHN-O-RAPID element analyzer (Weser, 1983). Carbonate content ranges between 6.4 and 86.3 wt.% and is the major matrix component in all investigated sediments. Biogenic opal was analyzed by the automated wet leaching method of Müller and Schneider (1993) and reaches up to 17.7 wt.%. The mineralogy of the clay size fraction of our selected sediment samples was investigated by X-ray powder diffraction. Texture preparations of the centrifuged, decalcified and dried sediment were analyzed in a Phillips PW 1820 diffractometer ($\text{Co K}\alpha$) and modeled with the Mac Diff 4.2.3 computer program by Petschick (2000). Iron and other element contents were identified with an automated X-ray fluorescence half-core (XRF) scanner (Jansen et al., 1998). Relative element concentrations are given in counts per second with a range from potassium (K) to iron (Fe) (Röhl and Abrams, 2000).

Grain size distribution was analyzed on ultrasonically resuspended wet bulk sediment using a Fritsch Economy Analysette 22 laser particle sizer (Fritsch,

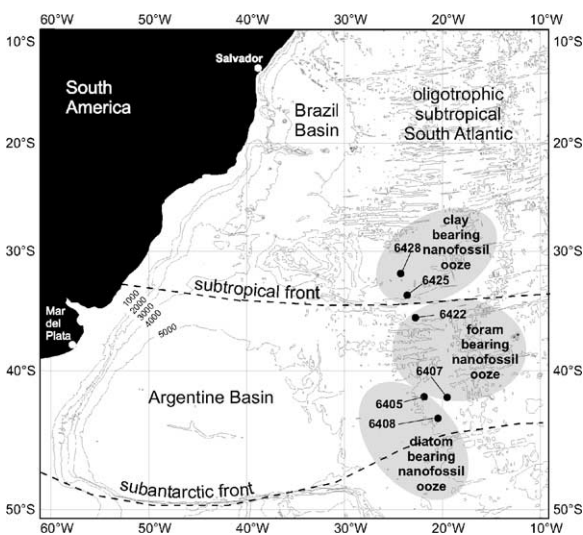


Fig. 1. Core locations in the subtropical and subantarctic South Atlantic on the western slope of the Mid-Atlantic Ridge. Sedimentation conditions are controlled by the frontal systems.

1994). This quick method yields a good representation of the fine sand and silt fraction, but systematically underestimates the submicron clay fraction (Konert and Vandenberghe, 1997). As this effect regards all sediments in a similar way, the obtained grain size fractions should nevertheless be valuable for differentiation.

For a combined paleo- and rock-magnetic analysis (Hofmann and Fabian, in preparation), NRM, IRM and ARM AF demagnetization curves were measured on cubic samples at 5 cm spacing using an automated 2G Enterprises 755 R pass-through cryogenic magnetometer. The issue of the best available NRM standardizer for paleointensity estimates has been widely discussed (Tauxe, 1993; Tauxe, 1995; Levi and Banerjee, 1976). IRM represents the concentration of all magnetic grain sizes. Susceptibility additionally includes the dia- and para-magnetic fraction. ARM, like PDRM, is linked to the fine magnetic particle spectrum as indicated by their similar coercivity spectra. In this study the RPI signals of the sediment samples were calculated by normalizing NRM with ARM after a 20 mT AF treatment to remove viscous overprints. The alternative normalizers yield similar signals except for core GeoB 6407-1.

Early diagenetic magnetite dissolution proceeds even under mildly suboxic conditions (Karlin and Levi, 1983; Canfield, 1989; Leslie et al., 1990). It affects especially the finest magnetite particles, the main carriers of PDRM, and leaves an imprint on the RPI records. Diagenetically affected core sections had to be excluded for the purpose of this study. They were identified by the magnetite dissolution index Fe/κ proposed by Funk et al. (2004). Stable plateau values of Fe/κ throughout the sediment column are indicative of unaltered magnetic mineralogy, while locally elevated values indicate partial magnetite losses due to reductive dissolution. The

rationale of this index is the diminution of the magnetic susceptibility κ relative to iron content caused by the diagenetic transformation of (ferric) ferrimagnetic into (ferrous) paramagnetic iron.

The Fe/κ plateau values of the investigated sediment cores increase by a factor of three from North to South (Franke, 2002). Two different Fe/κ levels were therefore applied to a northern (GeoB 6422-1, 6425-1, 6428-1) and southern (GeoB 6405-6, 6407-1, 6408-4) core group (Fig. 2), below which samples are considered as unaffected by reductive diagenesis. According to this criterion, more than one third of originally 90 samples gave subtle to pronounced indication of iron mineral reduction and was excluded from further consideration.

3. Results

The sedimentological characterization of the samples was based on analyses of the major components, grain size distribution and clay mineralogy. Ranges, means and N–S trends of all investigated parameters have been compiled as box-and-whisker plots in Fig. 3a–c. Foraminiferal and coccolithophorid carbonate make up 45–85% of the four northernmost cores and is complemented by terrigenous silicates (Fig. 3a). Temporal downcore variations are related to glacial-interglacial changes of the calcite lysocline (Schmieder et al., 2000). Near the subantarctic front, carbonate contents decrease 20–55% and give way to a much higher terrigenous content and additional siliceous components, mainly diatoms and radiolarians. In terms of the standard grain size classification 55–85% of the sediment falls into the

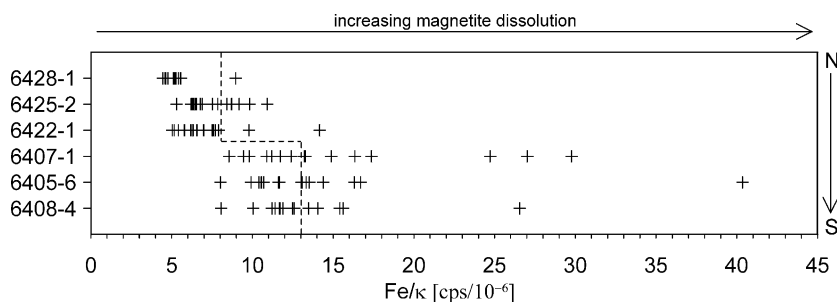


Fig. 2. Sample rejection based upon partial magnetic mineral dissolution according to regional Fe/κ criterion (Funk et al., 2004). Due to increasing Fe/κ plateau values from N to S, two separate threshold values for the northern and southern core group were chosen (dashed line).

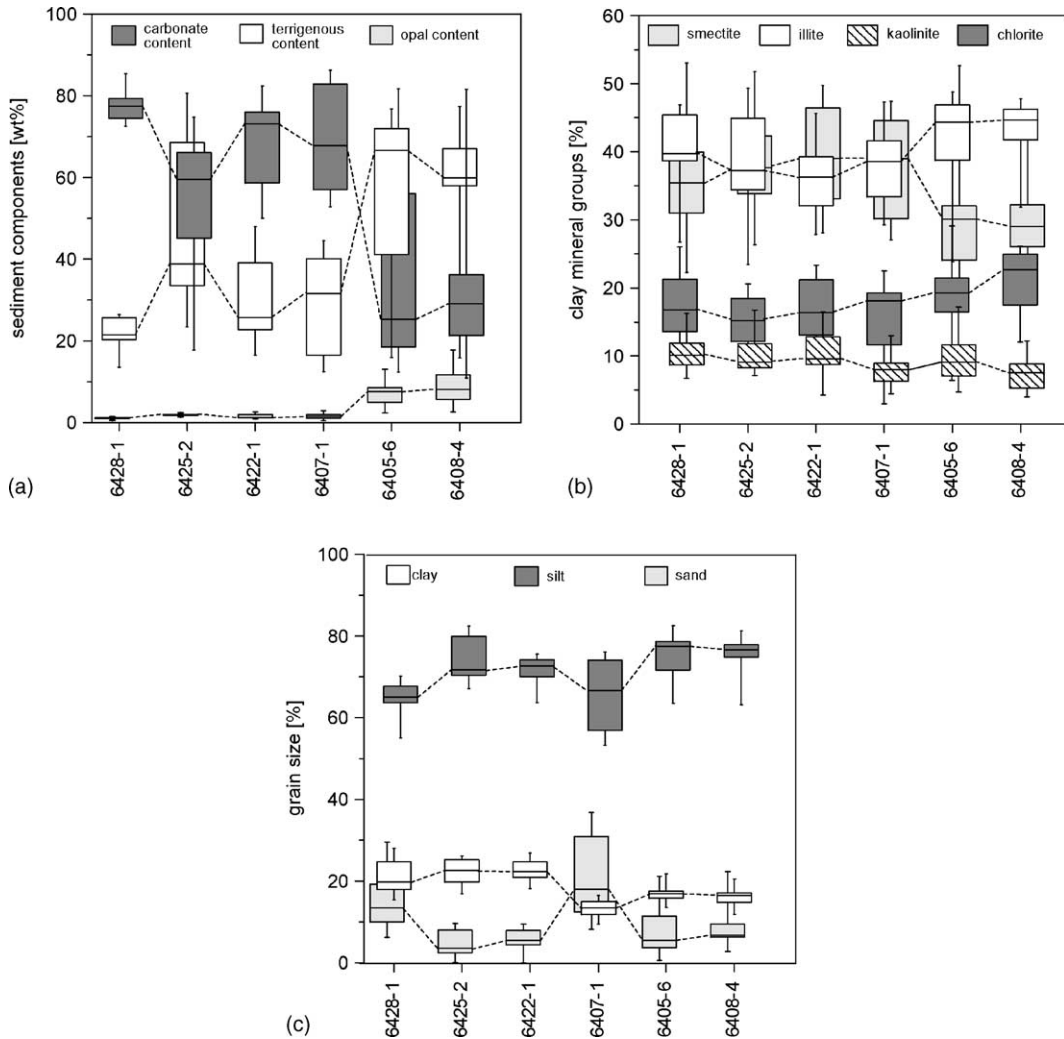


Fig. 3. Univariate box-and-whisker plots of (a) major components, (b) grain size distribution (c) clay mineralogy for the discrete samples from N to S. The boxes represent the median value and interquartile range; the whiskers mark the total data range.

silt fraction (2–63 μm), while sand (>63 μm) and clay (<2 μm) are subordinate (Fig. 3b). The terrigenous clay size fraction is higher in the subtropical than in the subantarctic zone. Winnowing effects explain the relatively high sand content at the shallowest site GeoB 6407-1 exposed to bottom-current erosion. The clay mineral analysis yields relative contents of the clay mineral groups smectite, illite, chlorite and kaolinite. Smectite and illite are the dominant phases and provide some 60–80% of the total content (Fig. 3c). In the subtropical zone, both minerals are nearly equally rep-

resented. The subantarctic region is characterized by a lower smectite and higher illite and chlorite content. Chlorite and kaolinite are subordinate, where chlorite is approximately twice as common as kaolinite. A source area and transport pathway of the clay minerals was investigated by Petschick et al. (1996).

All lithological parameters described above contribute to the sedimentary fabric and could be influential on PDRM acquisition. The dependency of the RPI values on each individual parameter was assessed on basis of a linear bivariate correlation analysis (Swan

and Sandilands, 1995). We take the standard approach in geostatistics and use Pearson's product-moment correlation coefficient

$$r_{xy} = \frac{\sum_{i=1}^n (x_i - \bar{x})(y_i - \bar{y})}{(N-1)s_x s_y}$$

where x_i are the independent sedimentological parameters, y_i the RPI values, \bar{x} and \bar{y} their respective means, s_x and s_y their standard deviations and N

the size of the statistical sample. The significance of any determined r_{xy} value, which may range from 0 (uncorrelated) to ± 1 (strictly linearly dependent), is controlled by the extent of the relationship r and by the number of cases N contributing to the analysis. The test statistics for significance of the correlation coefficient,

$$t = r \sqrt{\frac{N-2}{1-r^2}}$$

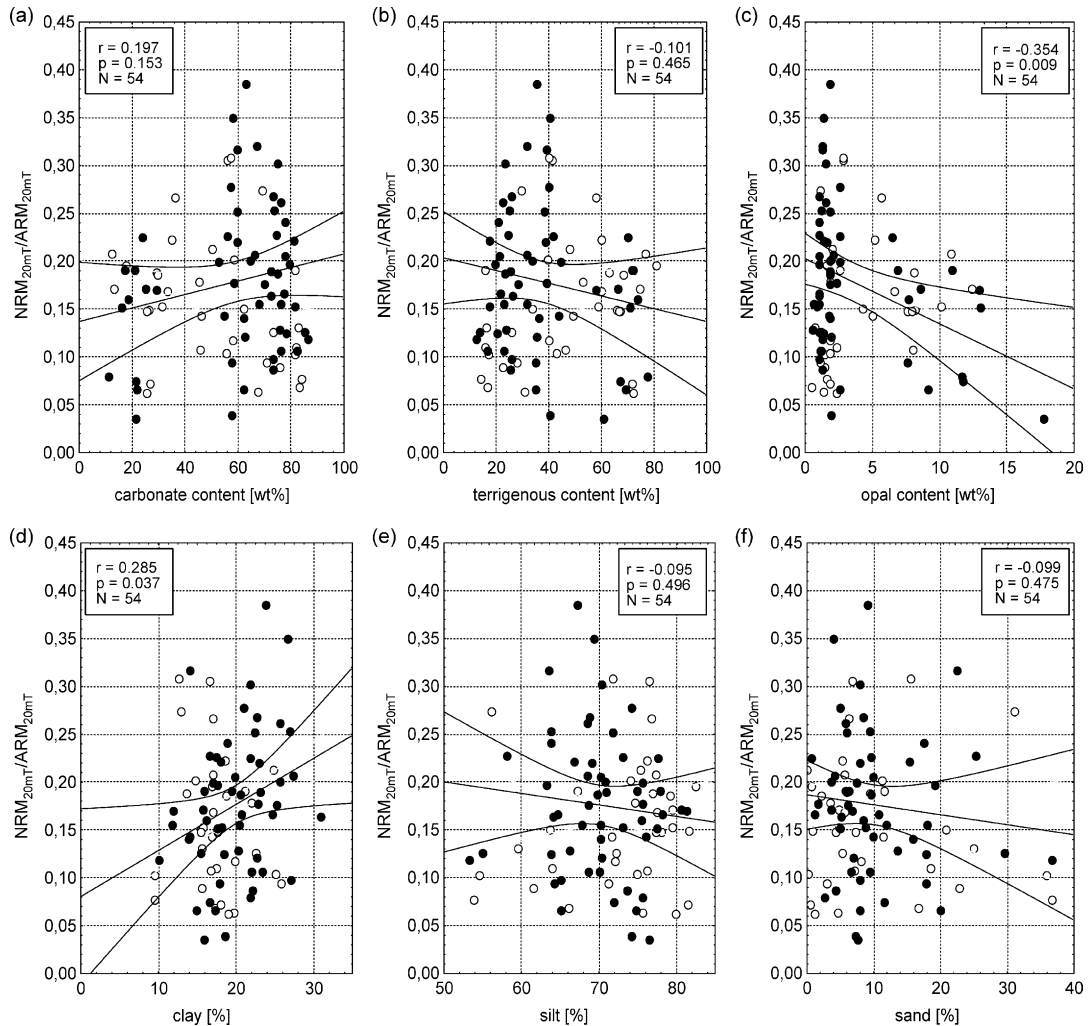


Fig. 4. Biplots of NRM_{20mT}/ARM_{20mT} vs. (a) carbonate, (b) terrigenous, (c) opal, (d) clay, (e) silt and (f) sand content. Pearson's correlation coefficients r , the probabilities p for randomness and samples sizes N are given in the figure headers. The gentle slopes of the regression lines and their broad 95% confidence range are indicative of large bivariate scatter. The correlations were exclusively based on the unaltered samples (solid symbols). The samples rejected by the diagenesis criterion (empty symbols) do not principally fall out of the major trend, but lower correlations and their significance.

leads to a probability measure, p , quantifying the likelihood, that an observed correlation is purely incidental. p -values of 0.05, 0.01 and 0.001 correspond to 95, 99 and 99.9% significance, respectively. Instead of using these fixed significance levels, we state the individual probability for randomness in each analysis.

The probability p is also reflected by the slope and width of the 95% confidence range of the linear regression line shown in the biplots. In contrast to the correlation coefficient r , the linear bivariate regression

calculation assumes a causal relationship between lithology and relative paleointensity and therefore minimizes the (squared vertical) deviation of the dependent variable, i.e. $\text{NRM}_{20\text{mT}}/\text{ARM}_{20\text{mT}}$. Because of the impact of geomagnetic field variations and the complexity of lithological controls, each individual sedimentological factor can only exert a partial and rather feeble influence on RPI. We therefore do not present each bivariate regression equation separately and give a multiple regression analysis below.

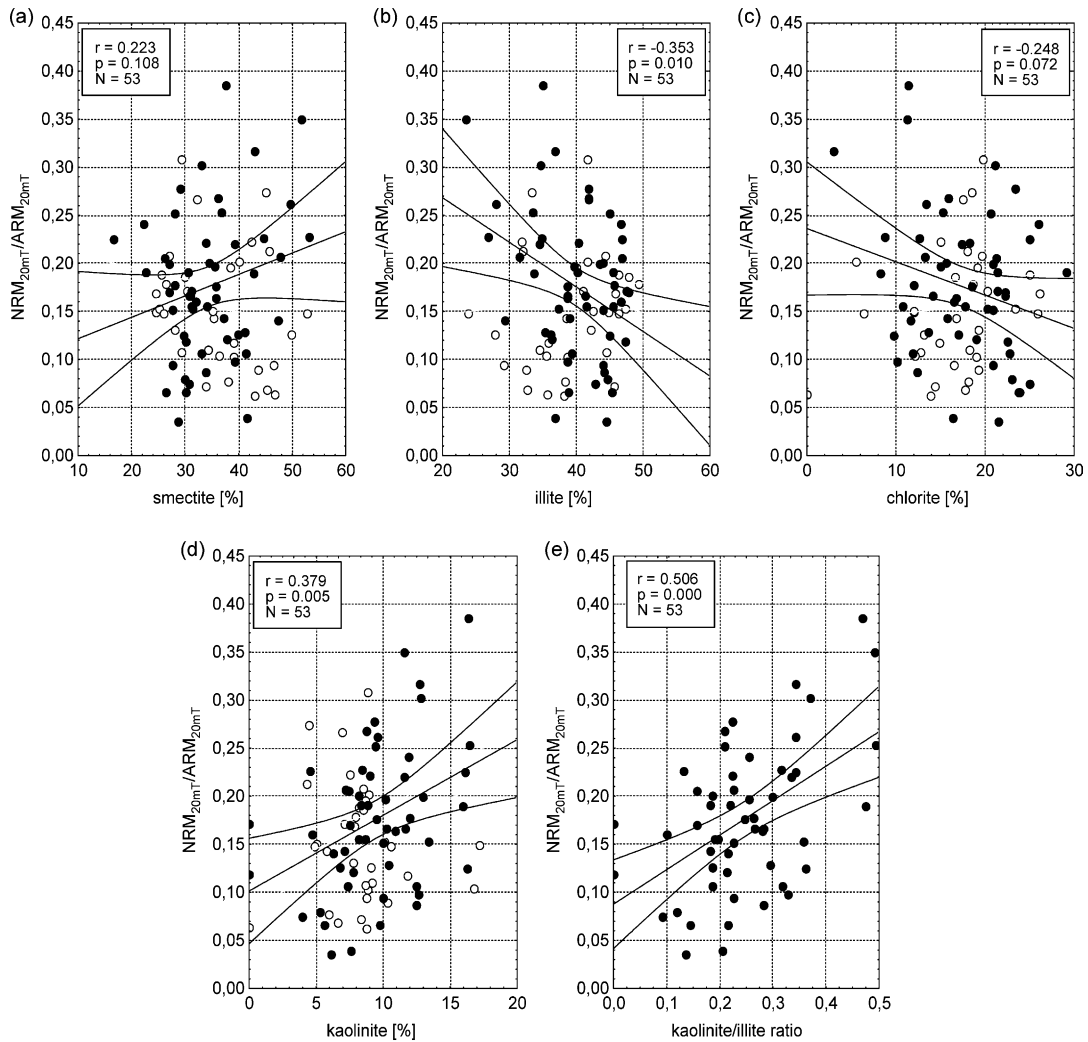


Fig. 5. Biplots of $\text{NRM}_{20\text{mT}}/\text{ARM}_{20\text{mT}}$ vs. (a) smectite, (b) illite, (c) chlorite, (d) kaolinite content and (e) kaolinite/illite ratio. For legends and symbols see Fig. 4.

For the following correlation analyses, the data of all 54 samples from the six cores were pooled to encompass a sufficiently large lithological variability and case number. The correlations of major components and grain size fractions with the NRM_{20mT}/ARM_{20mT} ratio are depicted in Fig. 4a–f. In four of the cases, carbonate and terrigenous content, silt and sand content, the correlations are practically insignificant. There is a low ($r = 0.29$) positive correlation with clay at significance level of about 97% and a moderate ($r = -0.35$)

negative correlation with opal content at 99% significance level. Fig. 5a–e show the correlations of relative clay mineral contents with the NRM_{20mT}/ARM_{20mT} ratio. In the case of smectite, the correlation is insignificant, while chlorite shows a low ($r = -0.25$) negative correlation at about 93% significance. Illite ($r = -0.35$) and kaolinite ($r = 0.38$) contents are moderately correlated with NRM_{20mT}/ARM_{20mT} , at significance levels of $\sim 99\%$. Because of the inverse relationships with kaolinite and illite, their ratio is more strongly

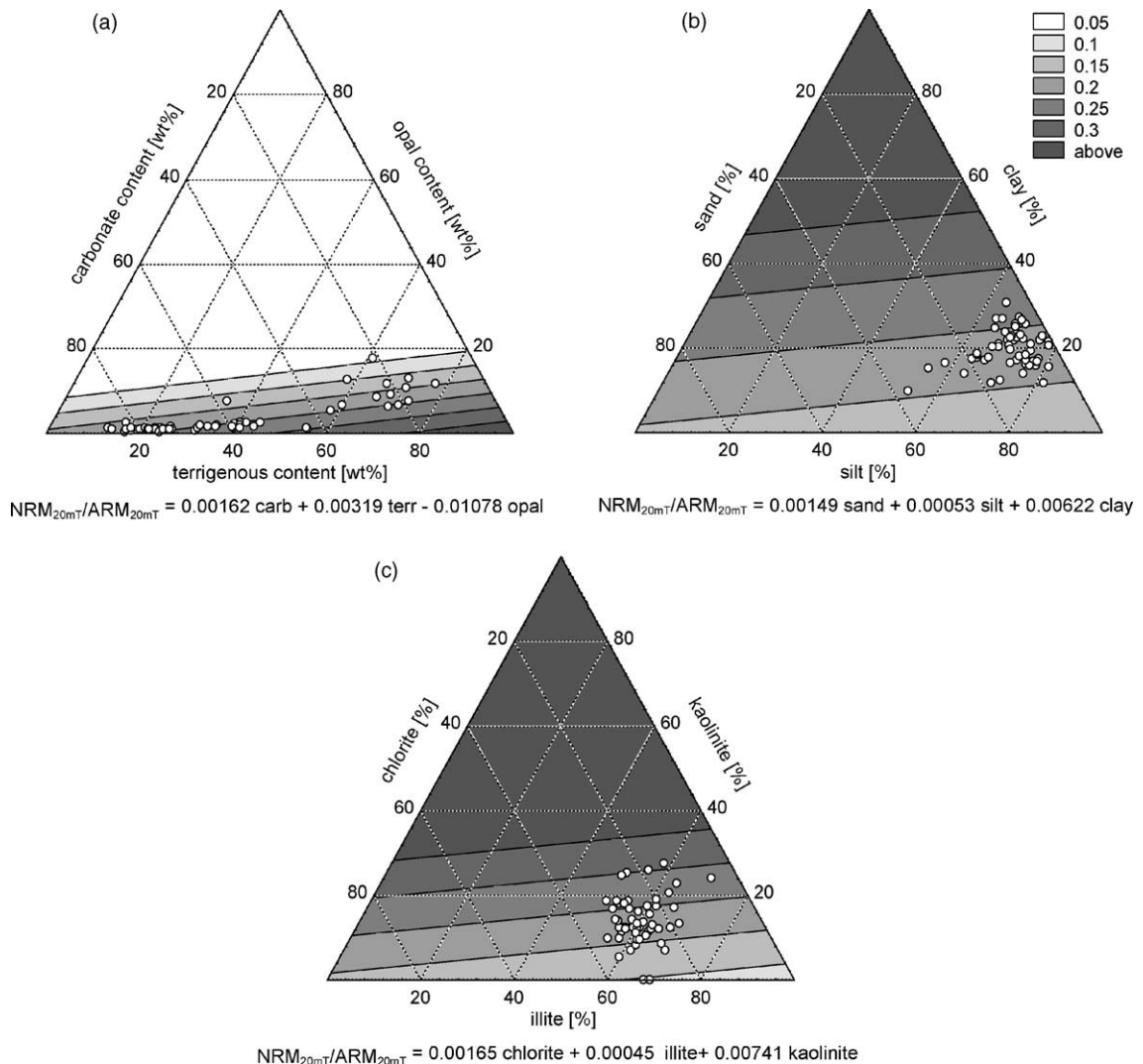


Fig. 6. Trend surface plots of NRM_{20mT}/ARM_{20mT} in the ternary systems of (a) carbonate, opal and terrigenous content, (b) sand, silt and clay percentage, (c) chlorite, illite and kaolinite.

($r = 0.51$) and significantly (>99.9%) correlated with NRM_{20mT}/ARM_{20mT} than either single value.

The three lithological parameter groups can be formulated as ternary systems, in which the observed NRM_{20mT}/ARM_{20mT} values are approximated by a regression plane (Fig. 6a–c). In the case of clay mineralogy, the apparently insignificant mineral smectite was excluded and the analysis was performed in the kaolinite–illite–chlorite system. The compilation of all three ternary plots clearly hints at the decisive factors. Rather small opal content seems to lower the RPI signal, while clay content and particularly the relative kaolinite content raise its value. The defining equations of the three ternary planes are given in the diagrams.

The bivariate analyses indicate that several of the investigated sedimentological parameters show a moderate but significant correlation with the RPI signal. Since all of these parameters are to some degree mutually independent, a multiple linear regression model of all factors can be established which quantifies the combined lithological controls on the RPI signal. The difficulty of distinguishing between meaningful and redundant parameters is a well-known problem (Swan and Sandilands, 1995). Here we use the ‘backward elimination’ method by which an initially overdetermined regression model is successively depleted from regressors with insignificant partial correlation. Multicollinearity is avoided by omitting at least one within a group of complementary parameters from the analysis. With reasonable settings, a multiple regression solution based on the three lithological parameters opal content, terrigenous content and kaolinite/illite ratio was found. The significance level of each individual regressor is equal to or better than 95% (Table 2). The goodness-of-fit R number is 0.59 and the probability of non-randomness exceeds 99.99%. The impact of lithology on RPI is demonstrated in Fig. 7. As the NRM_{20mT}/ARM_{20mT} record doubtlessly holds consid-

$$NRM_{20mT}/ARM_{20mT} = -0.009 \text{ opal} + 0.002 \text{ terrigenous} + 0.316 \text{ kaolinite/illite} + 0.068$$

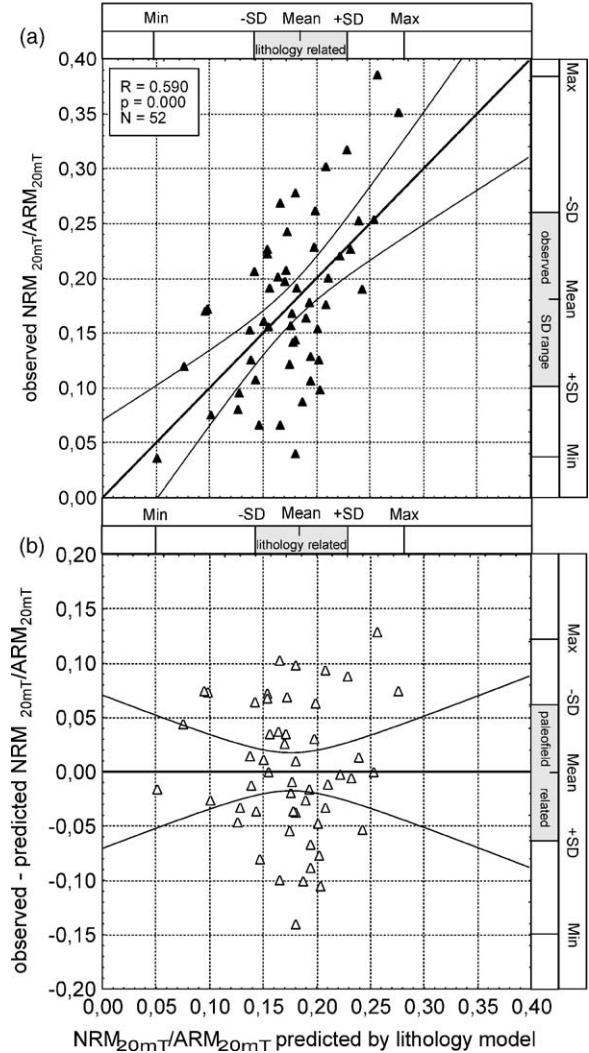


Fig. 7. Biplots of (a) observed and (b) residual NRM_{20mT}/ARM_{20mT} vs. predicted NRM_{20mT}/ARM_{20mT} resulting from the multiple regression model given above. Goodness of fit R , significance level p and sample size N is given in the figure header. All axes are equally scaled. Standard deviation (SD) ranges of the three shown parameters outline the average contributions of lithology and paleofield to the observed RPI signal.

Table 2
Summary of multiple linear regression analysis using the ‘backward elimination’ method

Regressors	Regression coefficient	SD of coefficient	P-Level
Intercept	0.068	±0.034	0.052
opal content	−0.009	±0.004	0.015
Terrigenous content	0.002	±0.001	0.031
Koalinite/illite ratio	0.316	±0.091	0.001

erable paleofield information, any better predictability solely based on lithological parameters would seem unrealistic.

As an alternative approach to quantifying lithology effects, the raw RPI (NRM_{20mT}/ARM_{20mT}) data of the

selected sediment samples were divided by isochronal values of the Sint-800 paleointensity stack. When plotted against the various lithology parameters, these ‘paleofield corrected’ RPI data show approximately the same scatter as the raw RPI data. It was initially expected, that correlations should be markedly improved by this data treatment. Probable causes for the failure are discrepancies in chronology and temporal resolution of the investigated and reference records.

4. Discussion and conclusions

Current quality requirements of RPI records as established by Levi and Banerjee (1976), King et al. (1983) and Tauxe (1993) are essentially based on rock- and paleomagnetic criteria, namely (1) magnetite as predominant magnetic carrier, homogeneity of (2) concentration and (3) magnetic grain size, as well as absence of (4) inclination errors and (5) magnetic mineral diagenesis. Ongoing analyses indicate, that criteria (1)–(4) are locally fulfilled by groups, the three northern and the three southern cores. Only for the pooled core set, the variations in magnetite concentration exceed the Tauxe (1993) ‘one order of magnitude’ rule. However, combining diverse lithologies was one basic requirement for the feasibility of this study. Criterion (5) was also respected: By rigorous application of the Fe/κ parameter all samples affected by (mild) chemical overprint, altogether one third of the initial collection, were excluded from the statistical analysis. What else influences paleointensity estimates?

Our statistical results suggest, that the sedimentary magnetic recording process of post-depositional particle alignment is not exclusively an expression of geomagnetic field history, but also controlled by the strong and complex interactions of magnetic carriers with their non-magnetic matrix. These mechanical and electrostatic forces are responsible for the relatively low intensity of PDRM in comparison with laboratory remanences such as ARM. The NRM_{20mT}/ARM_{20mT}

ratio of the investigated samples averages at around 0.18 (Table 3). The RPI signal dynamics due to varying matrix effects are considerable; if we compare the standard deviation (SD) range of the RPI data set (± 0.077) to the SD range of our lithology-dependent regression model (± 0.045) and to the paleofield-dependent residue (± 0.063), we find that matrix-related effects could possibly influence signal dynamics to nearly the same extend as geomagnetic field intensity variations.

Of course, the lithological spectrum encountered in our pooled sample set exceeds that of most published RPI records by far and therefore marks an upper limit of matrix-related signal biasing. Nevertheless, any paleointensity record claiming ‘high fidelity’ should additionally fulfil a criterion (6) related to lithological homogeneity, in particular with respect to clay mineralogy and major components. If RPI data are collected for stratigraphic purposes, we should expect sedimentologically induced patterns at lithological boundaries, e.g. at climate transitions. Our regression equations point towards the possibility of establishing multi-parameter based correction formulas to discard lithological overprint. A broader and more representative database such as the Sint-800 core set would be desirable for this objective. The numerous high-quality records should open the possibility to apply similar regression analyses on singular time slices sharpening the definition of the approach.

It is worth considering, why some of the sedimentological parameters seem to have greater influence on sedimentary magnetic recording than others. Our regionally restricted results indicate an inhibition of magnetic particle alignment by the presence of siliceous microfossils. This could be simply due to the porous structure of diatoms, radiolaria and sponge spicules which favor a high initial porosity followed by extreme postdepositional compaction. In addition, Florindo et al. (2003) suggested that magnetite alteration to authigenic smectite under oxic to suboxic conditions is favored by high silica concentrations. The growth of authigenic smectite directly on diatom

Table 3
Statistical properties of parameters in (Fig. 7)

Variable	Mean	Minimum	Maximum	SD
Observed NRM_{20mT}/ARM_{20mT}	0.183	0.035	0.385	0.077
Predicted NRM_{20mT}/ARM_{20mT}	0.183	0.049	0.281	0.045
Residual NRM_{20mT}/ARM_{20mT}	0.000	−0.153	0.126	0.063

Table 4
Comparative properties of common silicate clay minerals (adapted from Brady and Weil, 1996)

Property	Smectite	Illite	Kaolinite
Size (μm)	0.01–1.0	0.02–2.0	0.5–5.0
Shape	Flakes	Irregular Flakes	Hexagonal Crystals
External surface area (m^2/g)	70–120	70–100	10–30
Internal surface area (m^2/g)	550–650	–	–
Plasticity	High	Medium	Low
Cohesiveness	High	Medium	Low
Swelling capacity	High	Low to None	Low
Unit-layer charge	0.5–0.9	1.0–1.5	0
Interlayer spacing (nm)	1.0–2.0	1.0	0.7
Bonding	Van der Waal's	Potassium Ions	Hydrogen
Net negative charge (cmol_c/kg)	80–120	15–40	2–5

frustules has been described by Badaut and Risacher (1983). Clay mineralogy also appears to have a tight grip on magnetic particle orientation. We find that kaolinite has a positive and illite a negative effect on magnetic alignment, while smectite is more indifferent. This is certainly related to the unit-layer charges of the three clay minerals, eventually also to their crystalline versus flaky structure and low versus medium to high plasticity (Table 4). Specific investigations are needed to consolidate these hypotheses. We can nevertheless conclude, that lithology of the sedimentary matrix is an influential and widely underrated factor in the signal formation of relative paleointensity records.

Acknowledgements

Bernhard Diekmann from the Alfred-Wegener-Institute for Marine and Polar Research Bremerhaven/Potsdam was a great support for the clay mineral analyses. Rainer Petschick from Johann–Wolfgang Goethe University, Frankfurt a.M., kindly provided the ‘MacDiff 4.2.3.’ computer program for XRD analysis. Automated signal correlation for age modelling was performed with the unpublished computer programs ‘Automated Signal Correlation, v.07’ by Karl Fabian and ‘Correlation Tool, v.6’ by Thomas Frederichs from University of Bremen, Marine Geophysics group, to whom we owe also thanks for their support of the measurements. Monika Breitzke from GEOMAR Kiel supervised the laser granulometry. We thank Peter Müller for providing unpublished carbonate content data and Barbara Donner for unpublished $\delta^{18}\text{O}$ isotopy records. Financial support was provided by the

Deutsche Forschungsgemeinschaft (DFG), SPP 1097, in the framework of proposals Do 705/1-1 and Fa 408/1-2. Tilo von Dobeneck acknowledges a visiting research fellowship by the Netherlands Research Centre for Integrated Solid Earth Science (ISES). Christine Franke presently enjoys a stipend of the EUROPROX graduate college (Universities of Bremen, Utrecht and Amsterdam). All data presented in this study are available at the PANGAEA database (www.pangea.de, search string: FrankeC).

References

- Badaut, D., Risacher, F., 1983. Authigenic smectite on diatom frustules in Bolivian saline lakes. *Geochim. Cosmochim. Acta* 47, 363–375.
- Brady, N.C., Weil, R.R., 1996. *The nature and properties of soils*, 11th edition. Prentice-Hall International, Inc., New Jersey.
- Canfield, D.E., 1989. Reactive iron in marine sediments. *Geochim. Cosmochim. Acta* 53, 619–632.
- Creer, K.M., Morris, A., 1996. Proxy-climate and geomagnetic palaeointensity records extending back to ca. 75,000 BP derived from sediments cored from Largo Grande Di Monticchio. Southern Italy, *Quaternary Sci. Rev.* 15, 167–188.
- Florindo, F., Roberts, A.P., Palmer, M.R., 2003. Magnetite dissolution in siliceous sediments. *Geochim. Geophys. Geosyst.*, 4: 1053. doi: 10.1029/2003GC000516.
- Franke, C., 2002. *Der Einfluß der Lithologie auf die Rekonstruktion der “relativen Paläointensität” des Erdmagnetfeldes an spätquartären Sedimenten des subtropischen und subantarktischen Südatlantiks*, Diploma thesis, Department of Geosciences, University of Bremen, 117 pp.
- Fritsch GmbH Laborgerätebau, 1994. *Benutzer-Handbuch Laser Particle Sizer Analysette 22*, Idar Oberstein, pp. 30–37.
- Funk, J., von Dobeneck, T., Reitz, A., 2004. Integrated rock magnetic and geochemical quantification of redoxomorphic iron mineral diagenesis in Late Quaternary sediments from the

- Equatorial Atlantic. In: Wefer, G., Mulitza, S., Ratmeyer, V. (Eds.), *The South Atlantic in the Late Quaternary: reconstruction of material budgets and current systems*. Springer-Verlag, Berlin/Heidelberg/New York/Tokyo, pp. 239–262.
- Guyodo, Y., Valet, J.P., 1999. Global changes in intensity of the earth's magnetic field in the past 800 kyr. *Nature* 399, 249–252.
- Hofmann, D., Fabian, K., Schmieder, F., Donner, B., in preparation. A South Atlantic stratigraphic network.
- Hofmann, D. and Fabian, K., in preparation. Investigation of the relative paleointensity parameters with respect to lithological influences.
- Imbrie, J., Hays, J.D., Martinson, D.G., McIntyre, A., Mix, A.C., Morley, J.J., Pisias, N.G., Prell, W.L., Shackleton, N.J., 1984. The orbital theory of Pleistocene climate: support from a revised chronology of the marine $\delta^{18}\text{O}$ record. In: Berger, A.L., Imbrie, J., Hays, G., Kukla, G., Saltzman, B. (Eds.), *Milankovitch and climate*, 1. D. Reidel Publ. Comp, pp. 269–305.
- Jansen, J.H.F., Van der Gaast, S.J., Koster, A.J., 1998. CORTEX, a shipboard XRF-scanner for element analyses in split sediment cores. *Marine Geology* 151, 143–153.
- Karlin, R., Levi, S., 1983. Diagenesis of magnetic minerals in recent haemipelagic sediments. *Nature* 303, 327–330.
- Kent, D.V., 1982. Apparent correlation of paleomagnetic intensity and climate records in deep-sea sediments. *Nature* 299, 538–539.
- King, J.W., Banerjee, S.K., Marvin, J., 1983. A new rock-magnetic approach to selecting sediments for geomagnetic paleointensity studies: application to paleointensity for the last 4000 years. *J. Geophys. Res.* 88, 5911–5921.
- Konert, M., Vandenberghe, J., 1997. Comparisation of laser grain size analysis with pipette and sieve analysis: a solution for the underestimation of the clay fraction. *Sedimentology* 44, 523–535.
- Leslie, B.W., Hammond, D.E., Berelson, W.M., Lund, S.P., 1990. Diagenesis in anoxic sediments from the California Continental Borderland and its influence on iron, sulfur and magnetite behavior. *J. Geophys. Res.* 95B, 4453–4470.
- Levi, S., Banerjee, S.K., 1976. On the possibility of obtaining relative paleointensities from lake sediments. *Earth Planet. Sci. Lett.* 29, 219–226.
- Lu, R., Banerjee, S.K., Marvin, J., 1990. Effects of clay mineralogy and the electrical conductivity of water on the acquisition of depositional remanent magnetization in sediments. *J. Geophys. Res.* 95B, 4531–4538.
- Lu, R., 1992. A study of the effect of matrix properties on post-depositional remanent magnetization (pDRM) acquisition in sediments, Ph.D. thesis, University of Minnesota, 171 pp.
- Müller, P.J., Schneider, R., 1993. An automated leaching method for the determination of opal in sediments and particulate matter. *Deep-sea Res.* 1, 425–444.
- Nowaczyk, N.R., Harwart, S., Melles, M., 2001. Impact of early diagenesis and bulk particle grain size distribution on estimates of relative geomagnetic palaeointensity variations in sediments from Lama Lake, northern Central Siberia. *Geophys. J. Int.* 145, 300–306.
- Petschick, R., Kuhn, G., Gingele, F., 1996. Clay mineral distribution in surface sediments of the South Atlantic: sources, transport and relation to oceanography. *Marine Geology* 130, 203–229.
- Petschick, R., 2000. MacDiff 4.2.3, unpublished computer program, Johann-Wolfgang Goethe Universität, Frankfurt a. M.
- Roberts, A.P., Lehman, B., Weeks, R.J., Verosub, K.L., Laj, C., 1997. Relative paleointensity of the geomagnetic field over the last 200,000 years from ODP Sites 883 and 884, North Pacific Ocean. *Earth Planet. Sci. Lett.* 152, 11–23.
- Röhl, U., Abrams, L.J., 2000. High-resolution down hole and non-destructive core measurements from sites 999 and 1001 in the Caribbean Sea: application to the late Paleocene thermal maximum. In: Leckie, R.M., Sigurdsson, H., Acton, G.D., Draper, G. (Eds.), *ODP Sci. Res.*, 165, pp. 191–203.
- Swan, A.R.H., Sandilands, M., 1995. Introduction to geological data analysis. Blackwell Science Ltd., Oxford, London.
- Schmieder, F., von Dobeneck, T., Bleil, U., 2000. The Mid-Pleistocene climate transition as documented in the deep South Atlantic Ocean: initiation, interim state and terminal event. *Earth Planet. Sci. Lett.* 179, 539–549.
- Schmieder, F., 2004. Magnetic signals in Plio-Pleistocene sediments of the South Atlantic: chronostratigraphic usability and paleoceanographic implications. In: Wefer, G., Mulitza, S., Ratmeyer, V. (Eds.), *The South Atlantic in the Late Quaternary: reconstruction of material budgets and current systems*. Springer-Verlag, Berlin/Heidelberg/New York/Tokyo, pp. 263–279.
- Tauxe, L., Wu, G., 1990. Normalized remanence in sediments of the western equatorial Pacific: relative paleointensity of the geomagnetic field? *J. Geophys. Res.* 95B, 12.337–12.350.
- Tauxe, L., 1993. Sedimentary records of relative paleointensity of the geomagnetic field: theory and practice. *Rev. Geophys.* 31, 319–354.
- Tauxe, L., Shackleton, N.J., 1994. Relative paleointensity records from the Ontong-Java Plateau. *Geophys. J. Int.* 117, 769–782.
- Tauxe, L., 1995. Relative paleointensity in sediments: a pseudo-Thellier approach *Geophys. Res. Lett.* 22, 2885–2888.
- Valet, J.-P., Meynardier, L., 1993. Geomagnetic field intensity and reversals during the past four million years. *Nature* 366, 234–238.
- Verosub, K.L., 1977. Depositional and postdepositional processes in the magnetization of sediments. *Geophys. Space Phys.* 15, 129–143.
- von Dobeneck, T., Schmieder, F., 1999. Using rock magnetic proxy records for orbital tuning and extended time series analysis into the super- and sub-Milankovitch bands. In: Wefer, G., Fischer, G. (Eds.), *Use of proxies in paleoceanography: examples from the South Atlantic*. Springer-Verlag, Berlin/Heidelberg, pp. 601–633.
- Wefer, G. and cruise participants, 2001. Report and preliminary results of Meteor-cruise M 46/4, Mar del Plata (Argentina)—Salvador (Brazil), 10.2-13.3.2000, Reports of the Department of Geosciences, University of Bremen, 173, 136 pp.
- Weser, G., 1983. CHN-Elementanalyse im Halbmikromaßstab, Heraeus-Sonderdruck, Leybold-Heraeus GmbH, pp. 14–43.